

# Tectonic deformation of the Andes and the configuration of the subducted slab in central Peru: results from a microseismic experiment

G. Suárez,<sup>1</sup> J. Gagnepain,<sup>2</sup> A. Cisternas,<sup>3</sup> D. Hatzfeld,<sup>4</sup> P. Molnar,<sup>5</sup> L. Ocola,<sup>6</sup> S. W. Roecker<sup>7</sup> and J. P. Viodé<sup>3</sup>

<sup>1</sup> Instituto de Geofísica, Universidad Nacional Autónoma de México, México DF 04510

<sup>2</sup> Institut de Physique du Globe, Université de Paris VI, 4 Place Jussieu, 75006 Paris, France

<sup>3</sup> Institut de Physique du Globe, 5 rue René Descartes, 67084 Strasbourg Cedex, France

<sup>4</sup> Laboratoire de Géophysique Interne et Tectonophysique, Université Pierre Fourier, Saint Martin d'Heres, France

<sup>5</sup> Department of Earth, Atmospheric, and Planetary Sciences, MIT, Cambridge, MA 02139, USA

<sup>6</sup> Instituto Geofísico del Perú, Av. Higuiereta 577, Lima 33, Peru

<sup>7</sup> Rensselaer Polytechnic Institute, Department of Geology, Troy, NY 12180, USA

Accepted 1990 April 2. Received 1990 April 2; in original form 1989 April 21

## SUMMARY

A microearthquake survey was conducted in the central Andes of Peru, east of the city of Lima, to study the seismicity and style of tectonic deformation of the Peruvian Andes. Although most of the stations forming the temporary seismographic network were located on the high Andes, the vast majority of the microearthquakes recorded occurred to the east of the mountain belt: on the Huaytapallana fault in the Eastern Cordillera and beneath the western margin of the sub-Andes. Thus the sub-Andes appear to be the physiographic province subject to the most intense seismic deformation. Focal depths of the crustal events in this region range generally from 15 to 35 km and some events beneath the sub-Andes appear to be as deep as 40–50 km. The fault-plane solutions of events in the sub-Andean margin show thrust faulting on steep planes oriented roughly north–south, similar to that observed in teleseismic earthquakes studied using body wave modelling. The Huaytapallana fault in the Cordillera Oriental also shows relatively high seismicity along a NE–SW trend that agrees with the fault scarp and the east-dipping nodal plane of two large earthquakes that occurred on this fault on 1969 July 24 and October 1. Microearthquakes of intermediate depth recorded during the experiment show a flat seismic zone about 25 km thick at a depth of about 100 km. This agrees with recent observations showing that beneath Peru the slab first dips at an angle of about 30° to a depth of 100 km and then flattens following a quasi-horizontal trajectory. Fault-plane solutions of intermediate-depth microearthquakes have horizontal *T* axes oriented east–west suggesting slab pull is the dominant force in the downgoing slab.

**Key words:** Andes, microearthquakes, tectonics, Peru.

## INTRODUCTION

The west coast of South America is a major active margin where an oceanic plate is being subducted beneath a continental plate. It represents a contemporary example of the tectonic regime that is often presumed to have existed along the western margin of North America before the subduction of oceanic material ceased during the late

Cainozoic (e.g. Hamilton 1969; Atwater 1970). Thus, understanding the style of deformation and evolution of the Andes, an orogenic belt apparently uncontaminated by a continental collision, may play a crucial role in trying to decipher the complex tectonic history of previously active margins that are now dormant, or where an 'Andean' margin has been followed by a continental collision.

A useful tool to glean information about the style of

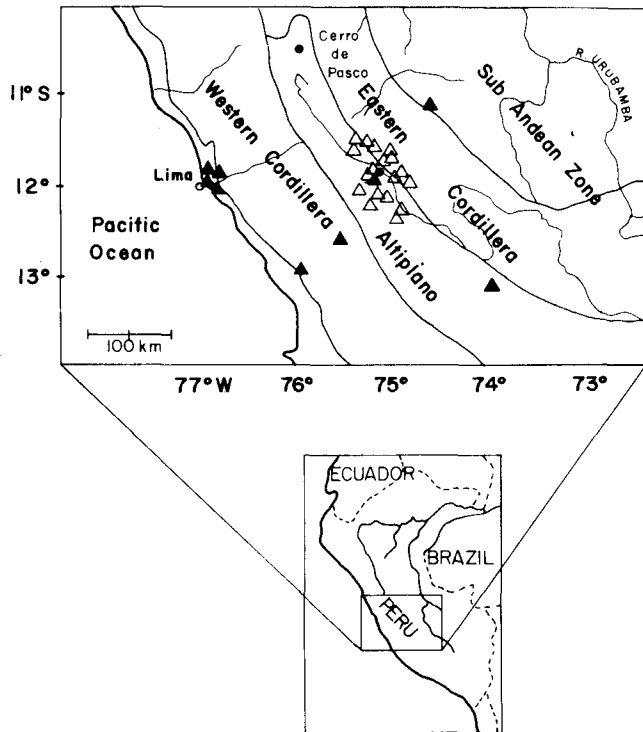


**Figure 1.** Solid lines show the boundaries of the main physiographic units of the central Andes of Peru (after Megard 1978). Open triangles show the location of the temporary seismographs; solid triangles are the stations of the permanent Peruvian Network.

deformation and tectonic regime of an active mountain belt is the study of the seismicity occurring within it. The spatial distribution of seismic activity indicates where brittle deformation is taking place, while the style of faulting inferred from fault-plane solutions allows inferences to be made on the orientation of the stresses responsible for this deformation. In the Andes, crustal seismic activity is low compared to that of the subduction zone to the west, and the routine determination of hypocentral locations published by the International Seismological Centre (ISC) and the United States Geological Survey (USGS) are not accurate enough for a detailed tectonic interpretation, due both to the poor geographical distribution of stations at teleseismic distances and the sparse coverage of the local stations; errors are specially large for focal depth determinations.

With the purpose of studying how the South American plate deforms due to the subduction of the Nazca plate to the west and to understand in more detail the morphology of the subducted slab beneath central Peru, a temporary network of portable seismographs was installed in the Altiplano and the Eastern Cordillera of the central Andes, east of the city of Lima (Fig. 1).

## METHOD OF ANALYSIS

A temporary network of up to 16 portable seismographs was installed in central Peru to complement the less dense permanent seismic network operated by the Instituto Geofísico del Perú (Fig. 1 and Table 1). Our goal was to monitor the seismic activity in the High Plateaus and the

**Table 1.** Station coordinates.

NAME	LAT	LONG	DELAY (sec)	LOCATION	ELEV (m)
ACO	-11.981	-75.095	0.08	ACOPALCA	3900
SAC	-11.778	-75.191	0.16	SACSACANCHA	4250
MAR	-11.604	-75.653	0.11	MARCAJASHA	4050
UNC	-11.235	-75.374	-0.36	UNCUSH	1925
COS	-12.140	-75.562	0.23	COSMOS	4600
CUL	-12.203	-75.211	0.06	CULHUAS	3800
LAI	-12.308	-75.359	0.07	LAIVE	3850
PAC	-11.778	-75.727	0.03	PACHACAYO II	3700
HYT	-11.960	-75.039	0.23	HUAYTAPALLANA	4600
PAM	-12.435	-74.870	0.04	PAMPAS	3750
PAG	-12.003	-74.917	0.01	PAGUA	3600
ATO	-12.341	-75.087	0.08	ATOMPAMPA	3900
MOL	-11.726	-75.409	0.02	MOLINOS	3650
PAR	-11.666	-75.085	0.12	PARCO II	3000
COC	-11.890	-75.305	-0.01	CONCEPCION	3500
COM	-11.699	-75.082	-0.12	COMAS	3000
YAU	-11.714	-75.469	-0.02	YAULI	3450
PAI	-11.782	-75.721	-0.03	PACHACAYO I	3700
PR1	-11.672	-75.083	-0.12	PARCO I	3000
VIS	-12.592	-74.961	0.12	VISCAPATA	4100
CHA	-12.011	-75.374	0.00	CHAMBARA	3350
GUA	-13.993	-75.789	-0.64	GUADALUPE	678
CAL	-12.627	-75.978	-0.42	CALACOCHA	1655
QUI	-12.943	-76.437	-0.68	QUILMANA	510
SJU	-15.356	-75.189	-0.77	SAN JUAN	75
NNA	-11.998	-76.843	-0.67	NANA	555
LM2	-12.068	-77.033	-0.67	LIMA2	127
HUA	-12.038	-75.323	-0.05	HUANCAYO	3313
VES	-12.213	-76.937	-0.77	V. EL SALVADOR	110
ANC	-11.775	-77.150	-0.78	ANCON	56
AYA	-13.080	-74.250	-0.17	AYACUCHO	2800
POC	-11.250	-74.600	-0.63	PTO OCOPA	750

Eastern Cordillera in the vicinity of the city of Huancayo (Fig. 1). The geographic coordinates and elevation above sea level of the portable stations were determined using topographical maps published by the Instituto Geográfico Militar of Peru at a scale of 1:100 000 (Table 1). We estimate the uncertainty in the location of the stations to be in the order of 250 m.

We used Sprengnether MEQ-800 seismographs with Mark Products L4-C vertical seismometers. The amplifiers were generally set to 84 dB, corresponding to a magnification of about  $5 \times 10^5$  at 10 Hz. Earthquakes were recorded on smoked paper at a speed of  $60 \text{ mm min}^{-1}$ . Records were changed every 48 hr and the drift of the internal clock of each instrument was checked at this same time interval by directly recording time pulses transmitted by the WWV station in Colorado, USA. Clock drifts during these 48 hr periods were always less than 0.1 s. The arrival times of the phases were digitized. The accuracy of the readings depended on the level of background noise and the sharpness of the onsets. On the average we estimate an accuracy of about 0.1 s for *P* arrival times. *S*-waves were also picked when they could be confidently identified, and we estimate the error in *S*-wave arrival times to be in the order of 1 s.

The earthquakes were located using the computer program HYOINVERSE developed at the USGS by Klein (1978). In the first iteration, *P* arrival times were generally assigned a weight of 1 and *S* arrival times a weight of 0.5. The smaller weights of the *S*-waves compensate the larger uncertainty in arrival-time readings of *S*-waves. The algorithm assigns weights to the observed arrival time as a function of the residual from the previous iteration. This is useful for damping arrival times that are grossly in error, as

in the case of misidentified phases. Arrival times showing large residuals were verified and reread.

A time correction (station delay) compensating for differences in elevation was applied to all arrival times at a given station (Table 1). The station corrections were applied assuming a reference elevation of 3500 m (the average elevation at the centre of the network) and assuming a mean  $P$ -wave velocity of  $5.0 \text{ km s}^{-1}$  for the top crustal layer.

## ACCURACY OF THE LOCATIONS

### Effects of the velocity structure

The velocity structure in central Peru is not well known. Although seismic refraction studies have been undertaken in southern Peru and northern Bolivia (e.g. Tatel & Tuve 1958; Ocola, Meyer & Aldrich 1971; Ocola & Meyer 1973), little work has been done in central Peru to constrain the velocity structure there. To examine the uncertainties in our locations due to our lack of knowledge of the velocity structure, we calculated the locations of several randomly selected events using three alternative velocity models (Table 2). The velocity structure inferred by Ocola & Meyer (1973) from a refraction survey across the Andes in southern Peru, that obtained by James (1971) from the dispersion of Rayleigh and Love waves along various paths in the Central Andes, and the velocity structure based on results of a deep, crustal refraction experiment carried out in Colombia by Meissner *et al.* (1977).

A total of 29 randomly selected earthquakes occurring at various depths were located using these three seismic velocity structures. The difference in epicentral coordinates and focal depths of these earthquakes are shown in histogram form (Fig. 2). In general, epicentral locations do not appear to depend strongly on the choice of the velocity structure; changes in epicentral coordinates are usually less

**Table 2.** Velocity models.

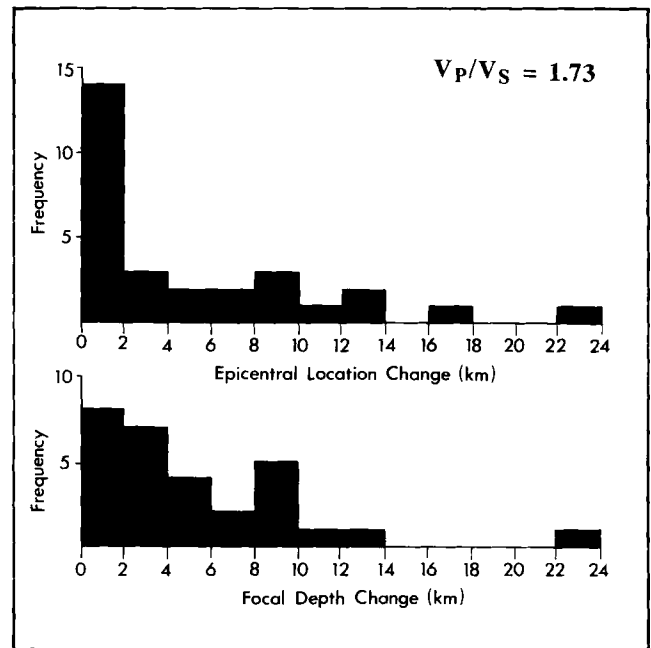
Ocola and Meyer (1975)	
$V_p$ (km/sec)	Depth to layer (km)
5.0	0.0
5.6	10.0
6.0	22.0
7.9	65.0
8.0	100.0

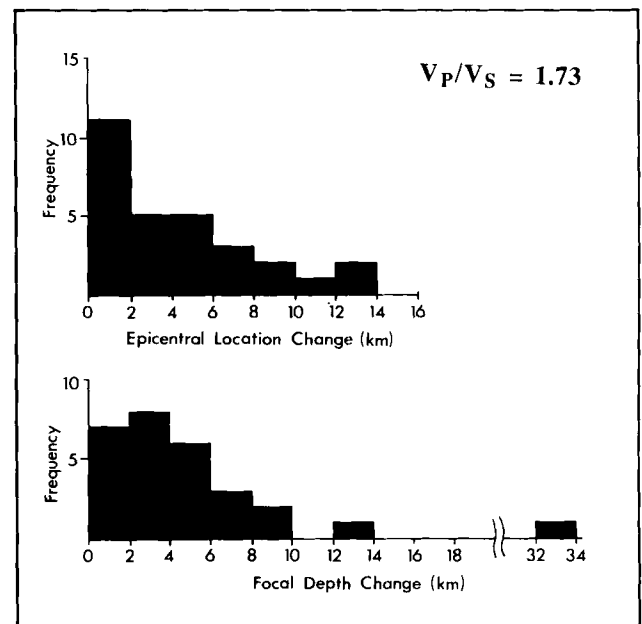
Meissner et al (1977)	
$V_p$ (km/sec)	Depth to layer (km)
5.9	0.0
6.2	10.0
6.7	30.0
8.1	50.0

James (1970)	
$V_p$ (km/sec)	Depth to layer (km)
5.0	0.0
6.0	8.0
6.6	25.0
7.9	60.0
8.0	100.0



a



b

**Figure 2.** (a) Histograms showing changes in calculated epicentres and focal depths for 29 events using the velocity structures proposed by Ocola & Meyer (1973) and James (1971) for the Central Andes. (b) Changes in calculated epicentres and focal depths for the same events using the velocity structures proposed by Ocola & Meyer (1973) and by Meissner *et al.* (1977) for southern Colombia.

than 4–6 km. Focal depths, however, are more sensitive to changes in the velocity structure and may vary by as much as 8–14 km depending upon the location of the event relative to the network. In both cases, however, earthquakes exhibiting large changes in epicentral location and focal depth ( $>10$  km) are events that lie outside of the network.

The velocity model obtained by Ocola & Meyer (1973) generally produced the smallest root-mean-square (rms) values of traveltimes residuals and was adopted to locate all of the events. A ratio of  $V_P/V_S$  of 1.73, corresponding to a Poisson's ratio of 0.25 was used in all cases. A variation in the ratio of  $V_P/V_S$  by about 0.3 produces changes in hypocentral locations that are usually not larger than 2 km (e.g. Chatelain *et al.* 1980; Prevot *et al.* 1980; Trehú 1982).

#### The quality of hypocentre locations

A total of 344 earthquakes recorded during the experiment were located (Fig. 3). The events located span an area of about 400 by 400 km. Most of these are earthquakes in the sub-Andes, east of the Andean Cordillera. Seismically, the high Andes appear to be relatively inactive with the exception of a linear NW–SE belt of earthquakes near the Huaytapallana fault in the Eastern Cordillera (near 12°S, 75°W). Intermediate-depth events within the subducted Nazca plate were also located beneath the high Andes and the sub-Andes. Very few events, however, were recorded near the coast along the main thrust contact between the Nazca and the South American plates, possibly because this area is far from our network. The high Andes are defined as the main Andean cordillera standing above elevations of about 3000 m.

Many of the events lie outside the network and the

maximum azimuthal gap in recording stations is sometimes quite large. A criterion for judging the accuracy of hypocentral depth determination is that the distance from the event to the closest station should be less than or roughly equal to the focal depth. For most of the crustal earthquakes in the sub-Andes this is not the case as many of them lie outside of our network. Focal depths of most of the crustal events appear to be less than 35–40 km and the distance to the closest station is often as large as 100–150 km. Consequently, HYPOINVERSE assigned large errors to the epicentral coordinates (ERH) and focal depths (ERZ) of some of the events located in the sub-Andes. Therefore, it is necessary to establish criteria for separating well-located earthquakes from poor and unreliable locations. From tests made on the data set, such as those shown of Fig. 2, reliable locations are defined as those meeting the following criteria: (1) those for which a minimum of five arrival times, including at least one S phase, were used; (2) those for which the calculated errors in the horizontal (ERH) directions are less than 10 km; (3) earthquakes with rms traveltimes residuals of less than 0.5 s; and (4) focal depth is similar to the epicentral distance to the closest station reporting the event. The errors in the hypocentral parameters of earthquakes meeting these criteria are probably not larger than about 5–10 km. Of the 344 located events, only 114 events met these criteria (Fig. 4).

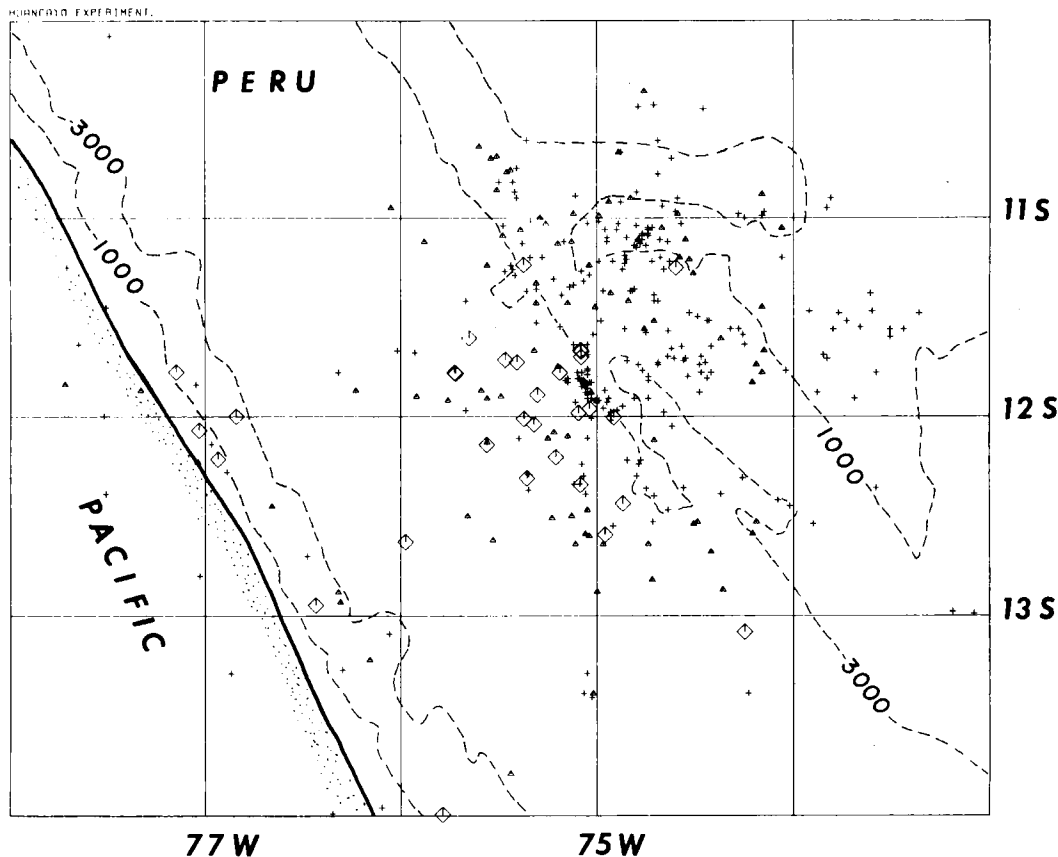


**Figure 3.** Epicentres of all 344 earthquakes recorded during the field experiment. Crosses indicate earthquakes with hypocentral depths shallower than 50 km, and the triangles events deeper than 50 km. Open diamonds show locations of stations used to locate the earthquakes. Dashed lines show the 1000 and 3000 m topographic contours of the Cental Andes.

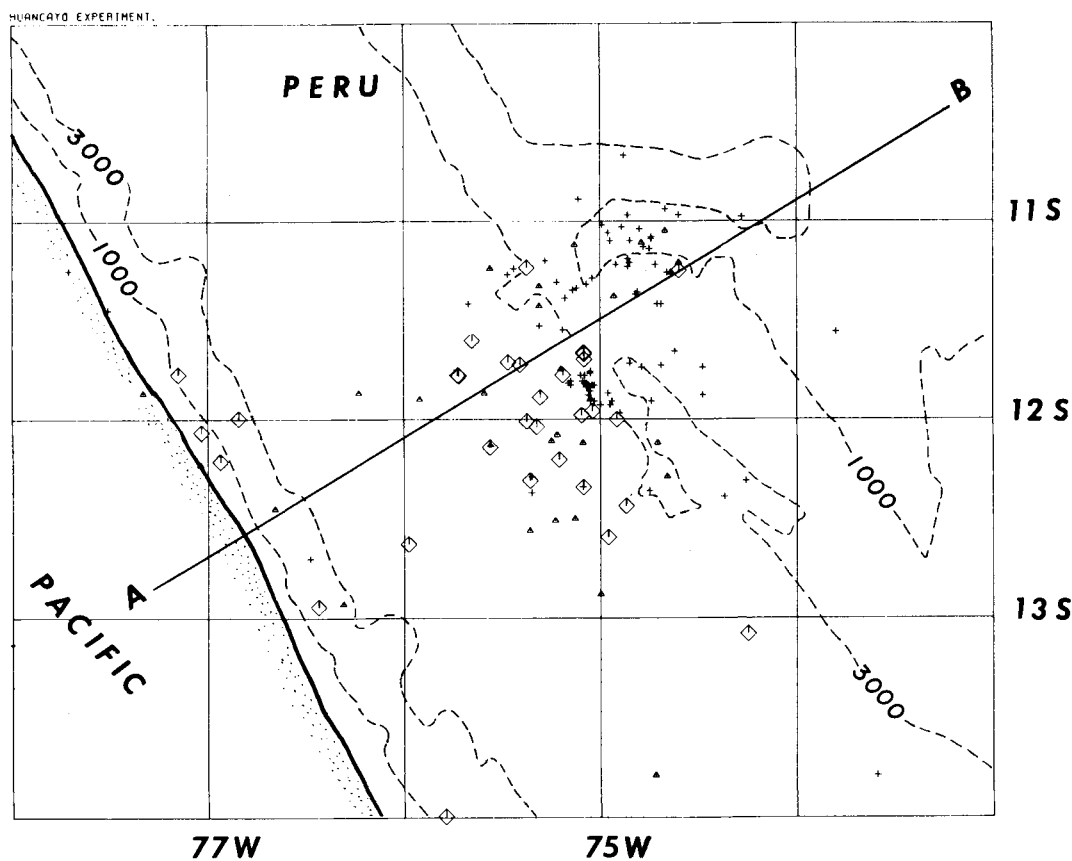


Figure 4. Epicentres of screened catalogue of well-located microearthquakes. Cross-section A-B is shown in Fig. 5. All symbols as in Fig. 3.

**SEISMICITY IN THE HIGH ANDES**

**Earthquakes in the Altiplano**

It is clear that crustal seismicity in the Altiplano is relatively low (Figs 3, 4, and 5). Although the majority of our portable stations were deployed in the western part of the

Altiplano, only 15 crustal earthquakes were located beneath the network; the overwhelming majority of crustal earthquakes occurred beneath the eastern margin of the Cordillera Oriental (Eastern Cordillera) and in the sub-Andes (Figs. 3 and 4). This pattern of seismicity is consistent with studies of teleseismically located events showing that most large, shallow events occur in the western

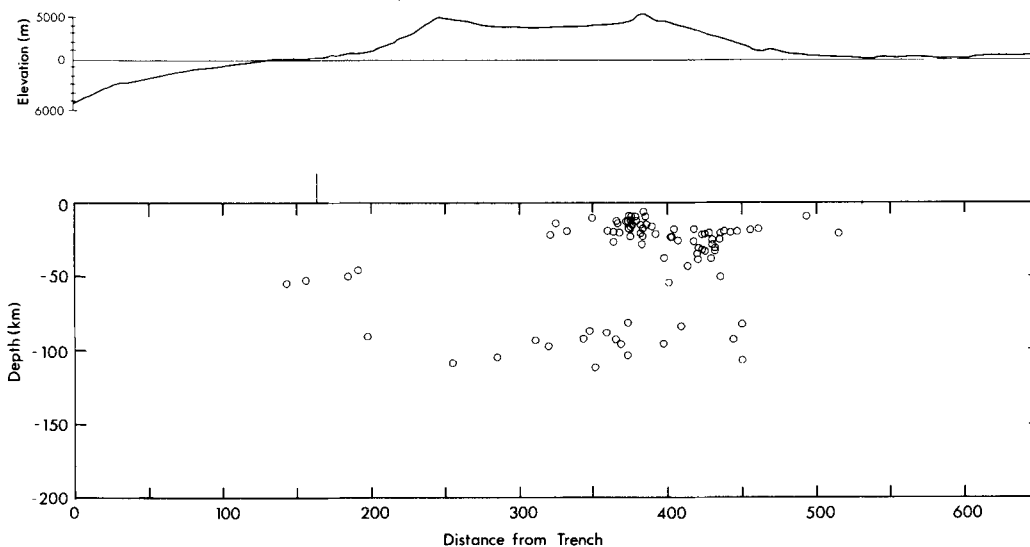


Figure 5. Open circles are the hypocentres of screened microearthquakes shown on Fig. 4, the cross-section A-B. Vertical tick mark on top of box shows location of coast line. Simplified topography of the Andes along the same cross-section is shown at the top.

part of the sub-Andes (e.g. Stauder 1975; Suárez, Molnar & Burchfiel 1983). Thus, the Altiplano appears to be rather stable, and not subject to orogenic deformation as intense as that affecting parts of the Eastern Cordillera and the whole of the western sub-Andes. Otherwise, the deformation must be either episodic with large periods of quiescence or absorbed by creep or viscoelastic behaviour. Reports of historical earthquakes and the location of teleseismic events do not support the former interpretation. Furthermore, crustal seismicity in the Peruvian Altiplano is also conspicuously absent of teleseismically located earthquakes since the installation of the worldwide networks in the early 1960s. A similar lack of seismicity is observed to the south, in the Bolivian Altiplano and the Argentinian Puna (Chinn & Isacks 1983), suggesting this observation made in the Peruvian Andes may be correlated to the rest of the Andean chain.

The few events that occurred in the Altiplano were all very small, and their fault-plane solution could not be obtained. Hence, it could not be confirmed whether normal faulting as that reported in the Cordillera Blanca of the high Andes in northern Peru (Dalmayrac 1974; Yonekura *et al.* 1979; Deverchere 1988) and in the Bolivian Altiplano (Lavenu 1978; Lavenu & Ballivian 1979; Mercier 1981) takes place in the Altiplano of Central Peru.

#### The Huaytapallana fault

The Huaytapallana fault is located in the Eastern Cordillera of Central Peru, 20 km east of the city of Huancayo (Fig. 1). Fault-plane solutions of two large earthquakes that occurred on this fault on 1969 July 24 and October 1 show reverse faulting with some strike-slip motion (Stauder 1975). The earthquake on October 1 produced a steep fault scarp dipping east, with a vertical displacement reaching 1.6 m (Deza 1971; Paredes 1972; Philip & Megard 1977). Philip & Megard (1977) interpreted this fault as forming part of a system of reactivated parallel faults trending NNW–SSE (Fig. 6).

The existence of a large number of small, shallow microearthquakes shows that the Huaytapallana fault (or system of faults) is still active. Station HYT, installed at the SE end of the mapped surface rupture, registered an average of about 30 events per day with  $S$ – $P$  time differences of less than 4 s (Fig. 6). The epicentres of earthquakes located in the vicinity of the Huaytapallana area follow a NNW–SSE trend, parallel to the mapped surface faults and to the strike of the east-dipping nodal plane of the fault-plane solutions of the two largest Huaytapallana earthquakes (Stauder 1975; Suárez *et al.* 1983) (Fig. 6).

Both the fault-plane solution of one of the largest microearthquakes and a composite fault-plane solution for four other events show reverse faulting with some left lateral strike-slip motion occurring on a fault plane dipping east with a strike of about 30° west of north (Fig. 7). This agrees with the sense of motion observed at the fault (Philip & Megard 1977) and with the fault-plane solution of the two large 1969 events.

Dollfus & Megard (1968) reported folding of Quaternary glacial moraines in the basins just west of the Huaytapallana fault. The strike of these folds, N30°W, and

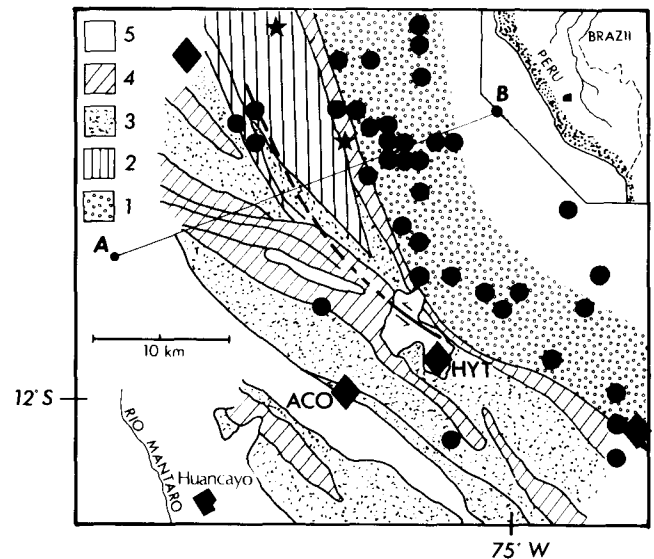


**Figure 6.** Epicentres of shallow earthquakes (filled circles) located in the vicinity of the Huaytapallana fault are shown plotted on a geological sketch-map of the Eastern Cordillera: (1) Precambrian gneisses; (2) Lower Palaeozoic flysch; (3) Upper Palaeozoic sedimentary rocks; (4) Triassic carbonates; and (5) Quaternary deposits. Filled diamonds represent the seismic stations and stars the epicentral locations of the 1969 July 24 and October 1 earthquakes as reported by the ISC. Solid line north of station HYT shows trend of fault scarp defined by Philip & Megard (1977); the dashed line is its inferred extension.

the orientation of the  $P$  axes of the fault-plane solutions of earthquakes in the Huaytapallana fault (Fig. 7), suggest that the region is being deformed by a regional, horizontal stress oriented roughly east–west, parallel to the direction of relative plate motion.

Philip & Megard (1977) studied a fault scarp approximately 3.5 km long. The total, approximate length of the fault responsible for the 1969 October 1 earthquake can be estimated from the formula  $M_0 = \mu u S$  (Aki 1966) using the following values. The average displacement ( $u$ ) observed on the fault scarp was 1.6 m (Philip & Megard 1977), the rigidity,  $\mu$ , is assumed to be  $3.3 \times 10^{11}$ , the observed fault width varies between 10 and 15 km, and the seismic moment is  $M_0 = 1.0 \times 10^{26}$  dyne cm (Suárez *et al.* 1983). From  $S$ , the area of the fault, we obtain a fault length of about 12–20 km for the October 1 earthquake depending on the fault width utilized. Thus, the 1969 event ruptured a fault that should extend north of the surface break observed by Philip & Megard (1977) to the region where the microearthquake activity occurs today (Fig. 6). This is confirmed by the fault scarp reported later by Sebrier *et al.* (1985) in that area.

The epicentres of most of the earthquakes recorded in this area lie about 10 km east of the projected surface location of the fault (Fig. 6). A cross-section across the fault shows that the depths of the earthquakes tend to increase towards the east (Fig. 8), consistent with an east-dipping fault plane. Unfortunately, the locations are not accurate enough to determine whether the earthquakes here take place on a single fault plane or on a series of imbricate sub-parallel faults.

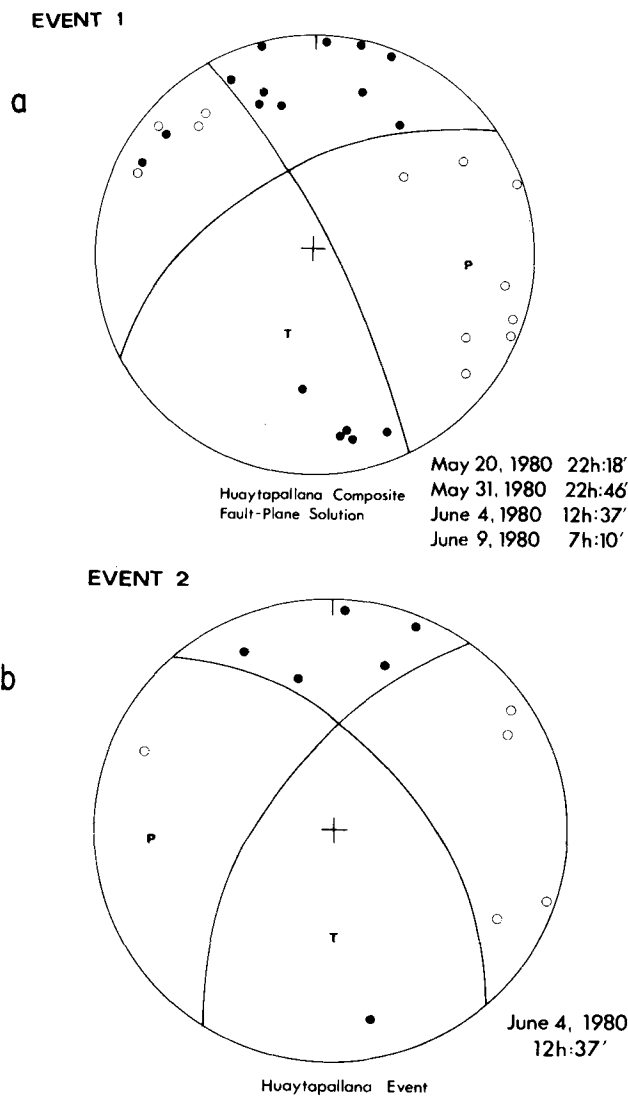


**Figure 7.** (a) Composite fault-plane solution of four earthquakes near Huaytapallana fault. (b) Single-event focal mechanism of earthquake located near the Huaytapallana fault. These are lower hemisphere equal-area projections. Open symbols indicate dilatation, closed symbols compression. Projection of axes is shown as *P* and *T*. Note both mechanisms are similar to that of the 1969 July 24 earthquake (Stauder 1975).

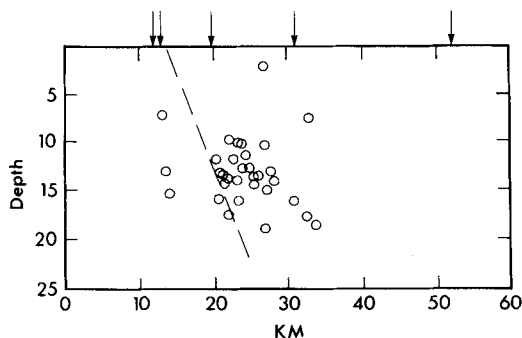


**Figure 8.** Hypocentres of the earthquakes near the Huaytapallana fault (open circles) projected onto cross-section A-B shown on Fig. 6. Vertical arrows indicate the position of the seismographic stations and the dashed line is the assumed dip of the Huaytapallana fault based on fault-plane solution of the 1969 events (Stauder 1975).

## SEISMICITY OF THE SUB-ANDES

### Description of the seismicity

The sub-Andes of central Peru are seismically more active than the high Andes and appear to be the physiographic province in the Peruvian Andes currently undergoing the most intense tectonic deformation. The vast majority of earthquakes in the overriding continental plate are concentrated in the sub-Andean region over an area roughly 100 km wide. These events lie east of the main Andean Cordillera, and occur beneath areas of relatively low topographic relief (Figs 3, 4 and 5). Teleseismic locations also show that throughout the Andes crustal seismicity is preferentially concentrated along the eastern piedmont of the mountain belt (Chinn & Isacks 1983; Suárez *et al.* 1983). Most of these events occurred at large distances from the eastern edge of the network and, therefore, their focal depths are poorly resolved. Station POC, operated by the Instituto Geofísico del Perú, is the only station located in the sub-Andes, but due to its low gain it could not be used to locate most of the microearthquakes that occurred in the area during the experiment.

There are enough well-located events in the western part of the sub-Andes to show that seismicity affects most of the crust here (Figs 4 and 5). The sub-Andean earthquakes are clearly concentrated within the upper 35 km, showing that brittle deformation extends here to abnormally large depths with respect to other intracontinental active belts (Fig. 5). Similar results were obtained by Dorbath *et al.* (1986) in an independent experiment. A few earthquakes in the sub-Andes were located at depths of between 40 and 50 km. This observation would imply that brittle deformation may involve the whole crust and perhaps part of the upper mantle. Nevertheless, these events are rare and their epicentres are outside of the seismic networks, showing relatively larger residuals ( $rms = 0.4$ ) than the better located earthquakes. Although these hypocentral locations are not of the best quality, it should be pointed out that a nearby large earthquake modelled using synthetic seismograms yields a focal depth of  $38 \pm 5$  km (Suárez *et al.* 1983). More data is necessary to confirm the extent of brittle seismic deformation in the sub-Andes and its implication in the tectonic evolution of Andean-type mountain belts.

### Fault-plane solutions and tectonic interpretation

A composite fault-plane solution from six events located just east of the network at depths of between 15 and 26 km shows thrust faulting with a component of strike-slip motion (Fig. 9a). This solution is very similar to that of the 1976 May 15 event that occurred 25 km to the east of this group of events at a depth of 20 km (Chinn & Isacks 1983; Suárez *et al.* 1983) (Fig. 10). Another fault-plane solution obtained for an event in the sub-Andes suggests nearly pure reverse faulting (Fig. 9b). Both of these solutions have the *P* axes oriented NE-SW, in a direction nearly perpendicular to the mountain range and parallel to the direction of relative plate motion (Fig. 10).

The existence of earthquakes in the sub-Andes at middle and lower crustal depths of between 20 and 35 km is unusual. In general, brittle deformation is confined to the top 15 km of the crust (Meissner & Strelhau 1982; Chen &

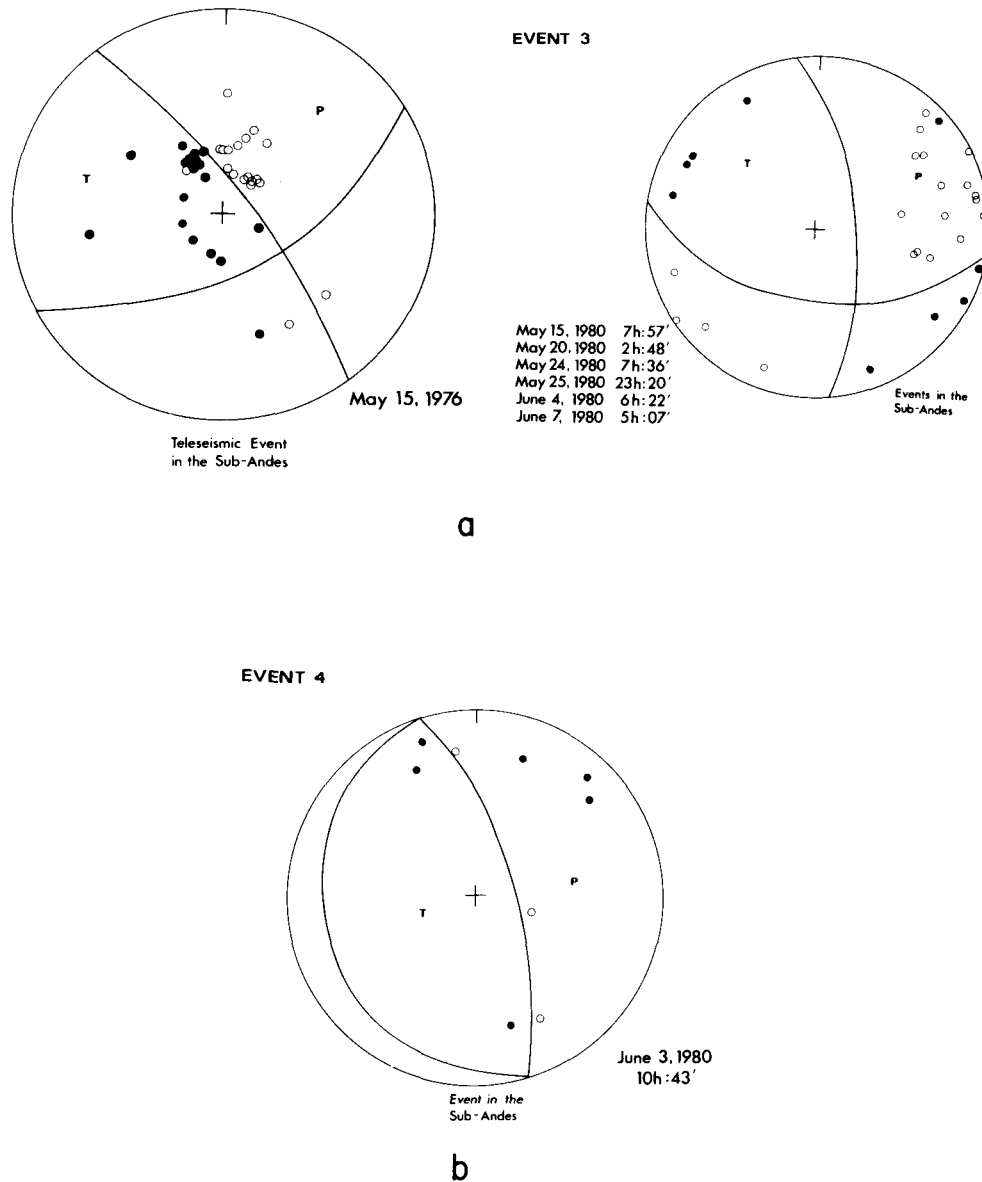


**Figure 9.** (a) Comparison of the composite fault-plane solution for six events in the sub-Andes with the fault-plane solution of the 1976 May 15 earthquake (Suárez *et al.* 1983) that was located about 20 km east of the events used in the composite solution. (b) Fault-plane solution of an earthquake located in the western sub-Andes. Symbols as in Fig. 7.

Molnar 1983). Below this depth, the absence of earthquakes is inferred to be due to the sharp decrease in strength of the typical crustal minerals under normal geothermal gradients (e.g. Brace & Kohlstedt 1980; Caristan 1982). To explain both the concentration of intense deformation along the western margin of the sub-Andes and the unusually deep seismic deformation, Suárez *et al.* (1983) suggested that the seismicity results from the underthrusting and deformation of the cold Brazilian shield beneath the eastern margin of the Cordillera Oriental.

Thus, it appears that the stresses applied to the western coast of the South American plate by the subduction of the Nazca plate are not deforming and elevating the Andean terranes that already have a high elevation. Instead, they seem to break and shorten the crust to the east where it is

probably thinner. This crustal shortening thickens the crust and progressively uplifts the topography of the Eastern Cordillera causing the Andean mountain range to grow eastward. In this scenario, the relatively deep microearthquakes and the large teleseismic events in the western sub-Andes probably reflect the tectonic deformation of the underthrust Brazilian shield (Suárez *et al.* 1983). This activity, however, is too far from our network and does not permit a more quantitative assessment.

The age and intensity of deformation of the sedimentary rocks in the sub-Andes is generally shown to decrease progressively to the east (Megard 1978; Dalmayrac, Laubacher & Marocco 1980) and may be interpreted as the result of the detached wedge of sedimentary rocks lying east of the zone of intense deformation in the western

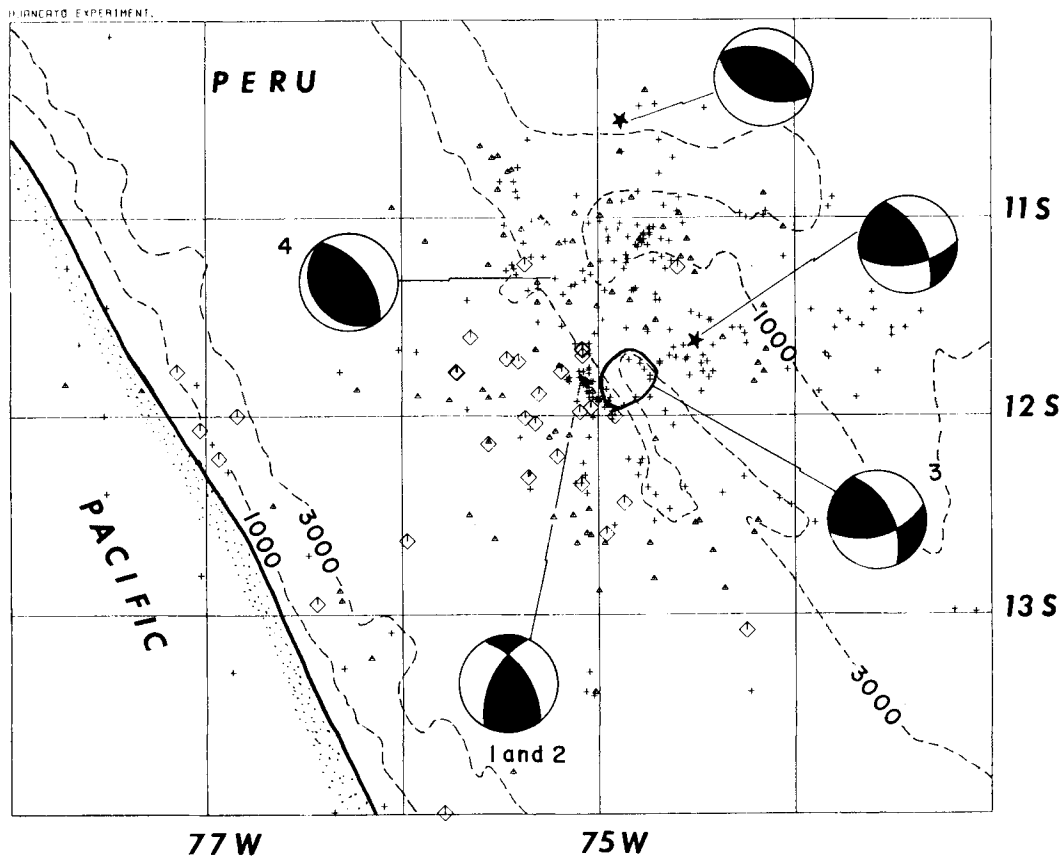


**Figure 10.** Map of the Central Andes summarizing lower hemispheric projections of fault-plane solutions of shallow crustal events obtained in this study. Dark quadrants are those showing compressional first motions. Numbers of fault-plane solutions correspond to event numbers in Figs 7 and 9. Also shown are the fault-plane solutions of two large events (stars) studied by Suárez *et al.* (1983) in this area. Other symbols as in Fig. 3.

sub-Andes. The large number of shallow microearthquakes occurring in the sub-Andes proper probably reflects the thin-skinned deformation of this accretionary prism.

### INTERMEDIATE-DEPTH EARTHQUAKES

Based on a selected catalogue of teleseismically located events, Barazangi & Isacks (1976, 1979) inferred that the seismic zone dips at about  $10^\circ$  beneath Peru. More recent results using earthquakes located by local networks in southern Peru (Hasegawa & Sacks 1981; Grange *et al.* 1984; Schneider & Sacks 1987) show that the seismic zone beneath central Peru dips initially at about  $30^\circ$  down to a depth of 100 km, and then flattens beneath western South America. During our field investigation we located 20 intermediate-depth earthquakes ranging in depth from 85 to 110 km with uncertainties of less than about 10 km. These earthquakes define a flat seismic zone about 25 km thick beneath the Andes and confirms that the seismic zone remains flat at a depth of about 100 km for at least a distance of 500 km from the trench (Fig. 5).

The fault-plane solutions determined for four of these intermediate-depth microearthquakes show normal faulting with  $T$  axes lying almost horizontally and parallel to the direction of relative plate motion (Figs 11 and 12). The

orientation of the  $T$  axes in the directions of the dip of the slab at intermediate depths in other subduction zones of the world has usually been interpreted as a result of the gravitational body force acting on the downgoing slab (Isacks & Molnar 1969).

Schneider & Sacks (1987) conclude that the horizontal  $T$  axes reflect the dominant slab-pull forces. Our results suggest that the seismic zone remains horizontal to a distance of about 500 km from the trench, where it appears to bend again and continue to greater depth with a relatively steep angle (Fig. 13). This interpretation is supported by the presence of a cluster of intermediate-depth events occurring at depths of about 150 km beneath eastern Peru (Fig. 13). Perhaps, a large number of earthquakes occur here because of the stresses produced by the forces bending the slab, in a situation analogous to that of a plate bent at a trench.

### CONCLUSIONS

A microseismic study of the Peruvian Andes east of the city of Lima was conducted during the summer of 1980 deploying a portable seismic network. The seismicity reveals that the most intense seismic deformation of this portion of the Peruvian Andes occurs in the western margin of the sub-Andes. The majority of the microearthquakes are located to the east of the main Andean Cordillera, beneath

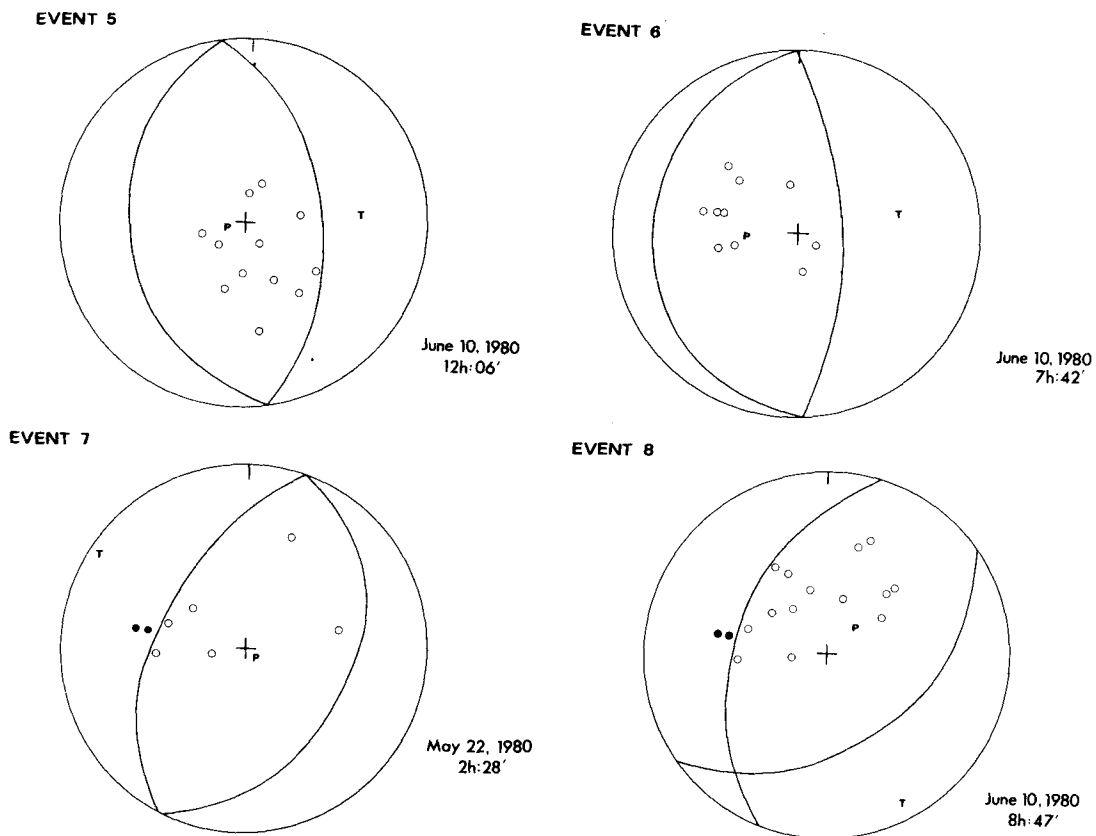


**Figure 11.** Fault-plane solutions of four intermediate-depth events recorded in this study. Symbols as in Fig. 7. Note *T* axes are nearly horizontal and oriented roughly east-west in all cases.

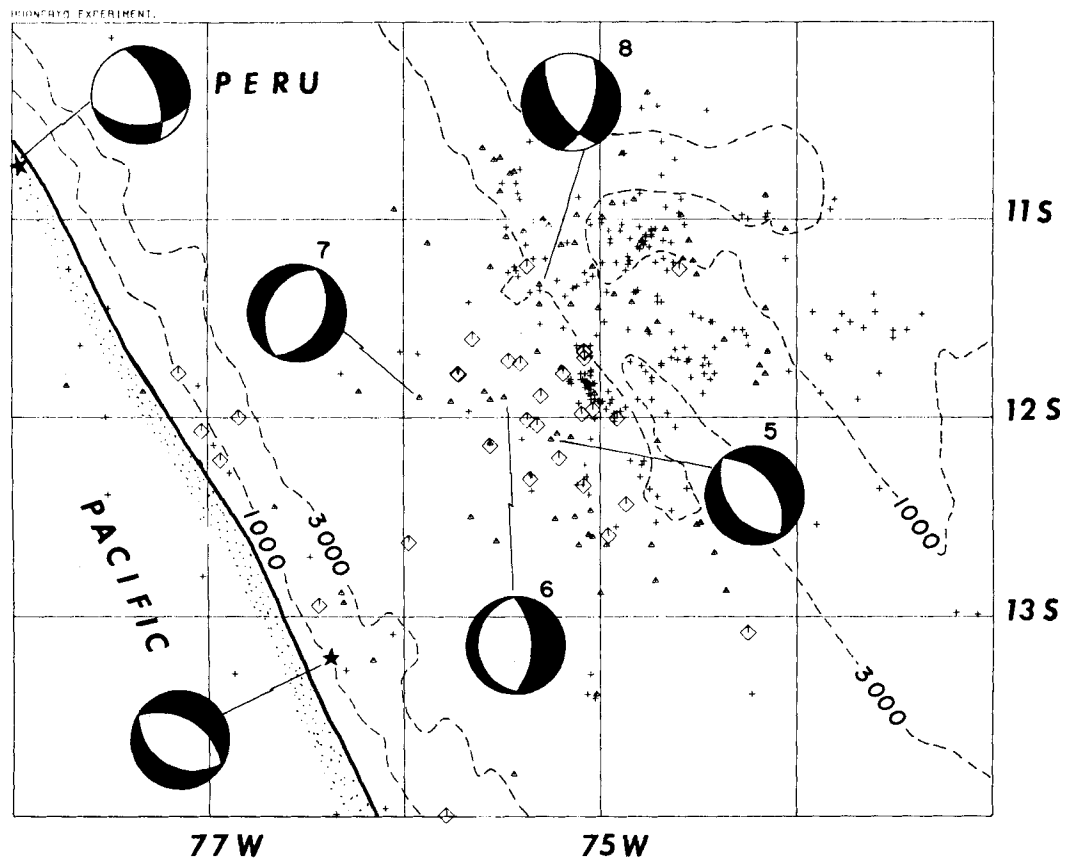


**Figure 12.** Map of central Peru summarizing lower hemisphere projections of the fault plane-solutions of intermediate-depth earthquakes obtained in this study. Numbers near fault-plane solutions correspond to event numbers shown in Fig. 11. Shown as stars are the locations and fault plane solutions of two intermediate-depth events studied by Stauder (1975). Dark quadrants indicate compressional first motions. Other symbols as in Fig. 3.

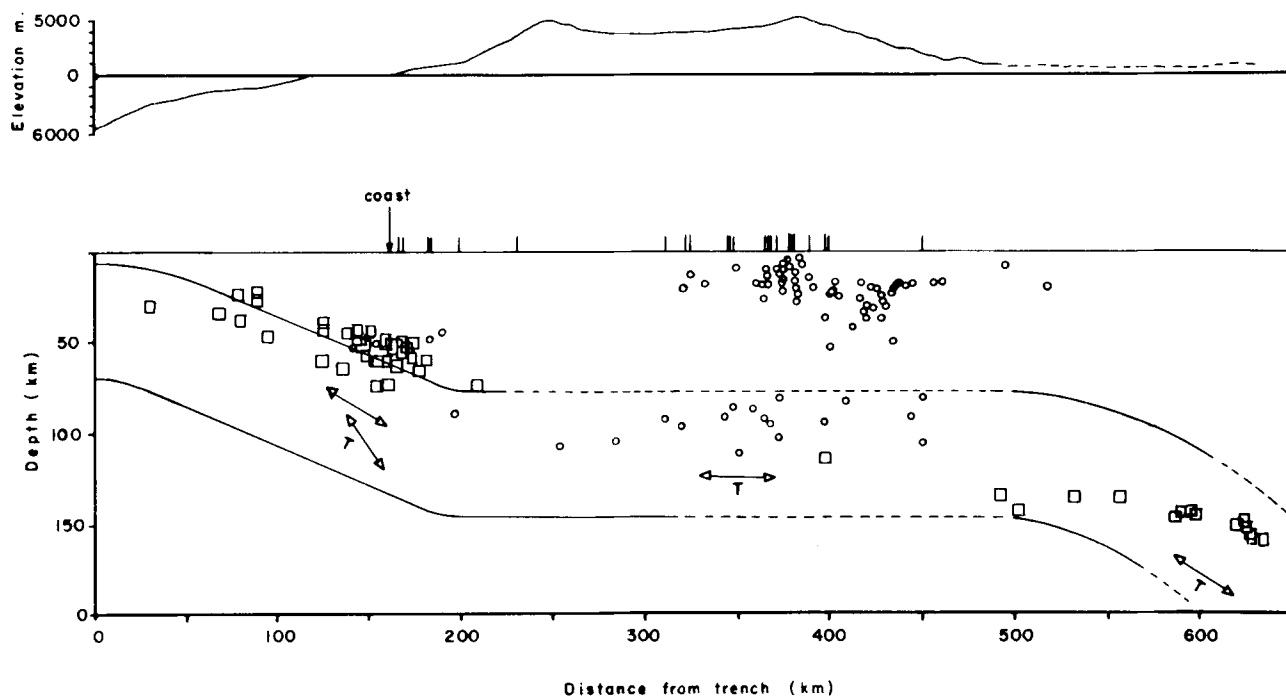


**Figure 13.** Cross-section approximately perpendicular to the coast line showing the inferred geometry of the subducted slab beneath Peru. To the earthquakes located in this study (shown as open circles) we have added the best located intermediate-depth events selected by Barazangi & Isacks (1976) in Peru (open squares). Tick marks are projected locations of the seismographic stations used in the experiment. Simplified topography is shown at the top of the figure. *T* axes of intermediate-depth events in this area are shown as arrows.

areas of low topographic relief. In the western margin of the sub-Andes the seismicity clearly reaches depths of about 35–40 km. The fault-plane solutions obtained for events in the western sub-Andes show high-angle reverse thrusting on planes oriented roughly north–south, coincident with the orientation of the stresses expected from the direction of relative plate motion. The results of the experiment are in agreement with the general features obtained from teleseismically located earthquakes in the Peruvian Andes suggesting the recorded microseismicity reflects current Andean orogenic process and may be extrapolated to other similar mountain belts.

The Altiplano appears to be relatively aseismic. In the high Andes, only the Huaytapallana fault in the Eastern Cordillera shows a high rate of seismic activity. Here, the fault-plane solutions of the microearthquakes are similar to those of the two large earthquakes that ruptured the fault in 1969. The microseismic activity in the vicinity of the Huaytapallana fault follows a trend parallel to mapped surface faults.

The intermediate depth even located range in depth from about 85 to 110 km. They define a flat seismic zone that underplates the Peruvian Andes horizontally up to a distance of 500 km from the trench. This is compatible with results obtained in southern Peru, which suggest that beneath Peru the slab dips initially at an angle of about 30° to a depth of 100 km and then flattens following a horizontal trajectory (Hasegawa & Sacks 1981; Grange *et al.* 1984; Schneider & Sacks 1987). The fault-plane solutions of the largest of these intermediate depth events show quasi-horizontal *T* axes oriented in the direction of relative plate motion.

## ACKNOWLEDGMENTS

We thank R. Benites, A. Flores, and F. Pardo for ably assisting us in the field, and D. Huaco, F. Megard, and M. Sebrier for their advice and help in logistics. We gratefully acknowledge the support provided by Ing. A. Giesecke, F. del Castillo, and J. Lanar at the Observatorio de Huancayo, Peru. This work was supported by NASA contract NAG5–300 at the Massachusetts Institute of Technology and a grant from the Institut National d’Astronomie et de Geophysique, France. Contribution no. 680 of the Institut de Physique du Globe, Paris.

## REFERENCES

- Aki, K., 1966. Generation and propagation of G waves from the Nigata earthquake of June 16, 1964, 2, Estimation of earthquake moment, released energy, and stress-strain drop from G wave spectrum, *Bull. Earthquake Res. Inst. Tokyo*, **44**, 73–88.
- Atwater, T., 1970. Implications of plate tectonics for the Cenozoic tectonic evolution of western North America, *Geol. Soc. Am. Bull.*, **81**, 3513–3536.
- Barazangi, M. & Isacks, B. L., 1976. Spatial distribution of earthquakes and subduction of the Nazca plate beneath South America, *Geology*, **4**, 686–692.
- Barazangi, M. & Isacks, B. L., 1979. Subduction of the Nazca plate beneath Peru: evidence from spatial distribution of earthquakes, *Geophys. J.R. astr. Soc.*, **57**, 537–555.
- Brace, W. F. & Kohlstedt, D. L., 1980. Limits on lithospheric stress imposed by laboratory experiments, *J. geophys. Res.*, **85**, 6248–6252.
- Caristan, Y., 1982. The transition from high-temperature creep to fracture in Maryland diabase, *J. geophys. Res.*, **87**, 6781–6790.

- Chatelain, J. L., Roecker, S. W., Hatzfeld, D. & Molnar, P., 1980. Microearthquake seismicity and fault plane solutions in the Hindu Kush region and their tectonic implications, *J. geophys. Res.*, **85**, 1365–1387.
- Chen, W. P. & Molnar, P., 1983. Focal depths of intracontinental and intraplate earthquakes and their implications for the thermal and mechanical properties of the lithosphere, *J. geophys. Res.*, **88**, 4183–4214.
- Chinn, D. S. & Isacks, B. L., 1983. Accurate source depths and focal mechanisms of shallow earthquakes in western South America and in the new Hebrides island arc, *Tectonics*, **2**, 529–563.
- Dalmayrac, B., 1974. Un exemple de tectonique vivante: les failles sub-actuelles du pied de la Cordillera Blanche (Perou), *Cah. ORSTOM, Ser. Geol.*, **6**, 19–27.
- Dalmayrac, B., Laubacher, G. & Marocco, R., 1980. Caracteres generaux de l'evolution geologique des Andes peruvienes, Travaux et Documents de l'ORSTOM, *Geologie des Andes Peruvienes*, Editions de l'Office de la Recherche Scientifique et Technique Outre-Mer, Paris, France.
- Deverchere, J., 1988. Extension crustale dans un contexte de convergence de plaques: L'exemple des Andes du Perou central contraint par ses données sismotectoniques, *These de Docteur en Science*, Université de Paris-Sud, Paris.
- Deza, E., 1971. The Pariahuanca earthquakes, Huancayo, Peru: July–October 1969, Recent crustal movements, *R. Soc. N. Z. Bull.*, **9**, 77–83.
- Dollfus, O. & Megard, F., 1968. Les formations quaternaires du bassin de Huancayo et leur neotectonique (Andes centrales peruvienes), *Rev. Geograph. Phys. Geol. Dynamique* (2), **X**, 5, 429–440.
- Dorbath, C., Dorbath, L., Cisternas, A., Deverchere, J., Diament, M., Ocola, L. & Morales, M., 1986. On crustal seismicity of the Amazonian foothill of the central Peruvian Andes, *Geophys. Res. Lett.*, **13**, 1023–1026.
- Grange, F., Hatzfeld, D., Cunningham, P., Molnar, P., Roecker, S. W., Suárez, G., Rodrigues, A. & Ocola, L., 1984. Tectonic implications of the microearthquake seismicity and fault plane solutions in southern Peru, *J. geophys. Res.*, **89**, 6139–6152.
- Hamilton, W., 1969. The volcanic central Andes — a modern model for the Cretaceous batholiths and tectonics of western North America, *Bull.* 65, pp. 175–184, Oregon Dept. Geology and Mineral Industries, Portland, OR.
- Hasegawa, A. & Sacks, I. S., 1981. Subduction of the Nazca plate beneath Peru as determined from seismic observations, *J. geophys. Res.*, **86**, 4971–4980.
- Isacks, B. & Molnar, P., 1969. Mantle earthquake mechanism and the sinking of the lithosphere, *Nature*, **223**, 1121–1124.
- James, D. E., 1971. Andean crustal and upper mantle structure, *J. geophys. Res.*, **76**, 3246–3271.
- James, D. E., 1978. Subduction of the Nazca plate beneath Central Peru, *Geology*, **7**, 174–178.
- Klein, F. W., 1978. Hypocenter location program Hypoinverse, *Open-file report* 78–694, United States Geological Survey, Menlo Park.
- Lavenu, A., 1978. Neotectonique des sediments plio-quaternaires du nord de l'Altiplano bolivien (Region de la Paz-Ayo-Umala), *Cah. ORSTOM, Ser. Geol.*, **X**, **1**, 115–126.
- Lavenu, A. & Ballivian, O., 1979. Estudios neotectónicos de las cuencas de las regiones de Cochabamba, Sucre, Tarija-Cordillera oriental boliviana, *Rev. Acad. Nac. Cien. Bolivia.*, **2**, 107–129.
- Megard, F., 1978. Etude géologique des Andes du Perou central, *Mem.* 86, Office de la Recherche Scientifique et Technique Outre-Mer, Paris, France.
- Meissner, R. & Strehlau, J., 1982. Limits of stresses in continental crusts and their relation to the depth-frequency distribution of shallow earthquakes, *Tectonics*, **1**, 73–89.
- Meissner, R. O., Flueh, E. R., Stibane, F. & Berg, E., 1977. Dinámica del límite de placas activo en el SW de Colombia de acuerdo a recientes mediciones geofísicas, in *Transición Oceano-Continente en el Suroests de Colombia*, pp. 169–198, eds Ramírez, J. E. & Aldrich, L. T., Instituto Geofísico-Universidad Javeriana, Bogota, Colombia.
- Mercier, J. L., 1981. Extensional-compressional tectonics associated with the Aegean Arc: comparison with the Andean Cordillera of south Peru-north Bolivia, *Phil. Trans. R. Soc. Lond.*, **300**, 337–355.
- Ocola, L. C. & Meyer, R. P., 1973. Crustal structure from the Pacific basin to the Brazilian shield between 12° and 30° south latitude, *Bull. seism. Soc. Am.*, **84**, 3387–3403.
- Ocola, L. C., Meyer, R. P. & Aldrich, L. T., 1971. Gross crustal structure under Peru-Bolivia Altiplano, *Earthquake Notes*, **42**, 33–48.
- Paredes, J., 1972. Etude géologique de la feuille de Jauja au 1 : 100 000 (Andes du Perou Central), *These 3eme Cycle*, Univ. Sci. Tech. Languedoc, Montpellier, France.
- Philip, H. & Megard, F., 1977. Structural analysis of the superficial deformation of the 1969 Pariahuanca earthquakes (central Peru), *Tectonophysics*, **38**, 259–278.
- Prevot, R., Hatzfeld, D., Roecker, S. W. & Molnar, P., 1980. Shallow earthquakes and active tectonics in Eastern Afghanistan, *J. geophys. Res.*, **85**, 1347–1357.
- Schneider, J. F. & Sacks, I. S., 1987. Stress in the contorted Nazca plate beneath southern Peru from local earthquakes, *J. geophys. Res.*, **92**, 13 887–13 902.
- Sebrier, M., Mercier, J. L., Mégard, F., Laubacher, G. & Carey-Gailhardis, E., 1985. Quaternary normal and reverse faulting and the state of stress in the central Andes of Peru, *Tectonics*, **4**, 739–780.
- Stauder, W., 1975. Subduction of the Nazca plate under Peru as evidenced by focal mechanisms and by seismicity, *J. geophys. Res.*, **80**, 1053–1064.
- Suárez, G., Molnar, P. & Burchfiel, B. C., 1983. Seismicity, fault-plane solutions, depth of faulting, and active tectonics of the central Andes, *J. geophys. Res.*, **10** 403–10 428.
- Tatell, H. E. & Tuve, M. A., 1958. Seismic studies in the Andes, *EOS, Trans. Am. geophys. Un.*, **39**, 580–582.
- Trehú, A. M., 1982. Seismicity and structure of the Orozco transform fault from ocean bottom seismic observations, *PhD thesis*, MIT — Woods Hole Oceanographic Inst.
- Yonekura, N., Matsuda, T., Nogami, M. & Kaizuka, S., 1979. An active fault along the western foot of the Cordillera Blanca, Peru, *J. Geog.*, Tokyo, **88**, 1–19.